Journal of Industrial and Management Optimization

https://www.aimspress.com/journal/jimo

JIMO, 22(3): 1491–1518.
DOI:10.3934/jimo.2026055
Received: 05 January 2026
Revised: 29 January 2026
Accepted: 05 February 2026
Published: 27 February 2026

Research article

Modeling the impact of uncertain demand on intracity express delivery network design by adjustable data-driven robust approach

Shijun Wang[1], **Yanjiao Wang**[2,*], **Naiqi Liu**[3] **and Weida Zhang**[1]

[1] School of Law and Public Administration, Hebei Normal University, Shijiazhuang 050024, Hebei, China

[2] Hebei Key Laboratory of Machine Learning and Computational Intelligence, College of Mathematics & Information Science, Hebei University, Baoding 071002, Hebei, China

[3] College of Management and Economics, Tianjin University, 300072, Tianjin, China

* **Correspondence:** Email: wangyanjiao@stumail.hbu.edu.cn.

Abstract: With the rapid development of e-commerce, intracity express delivery services have become an integral component of modern logistics systems while facing unprecedented challenges. This paper addresses the service network design problem for capacity-constrained intracity express delivery systems. We propose a two-stage decision framework wherein the first stage determines vehicle routing plans and calculates transportation costs, and the second stage arranges parcel transportation based on actual demand and evaluates the associated penalty costs. Recognizing the uncertainty in demand inherent to real-world operations, this paper specifically examines how demand fluctuations affect system performance. To address this challenge, we construct an uncertainty set using support vector clustering (SVC) based on available historical data, which serves as the foundation for developing a data-driven adjustable robust optimization (ARO) model. Through linear decision rules and conic optimization theory, we transform the robust model into an equivalent mixed-integer linear programming formulation and develop a customized Benders dual decomposition algorithm for its solution. The proposed methodology is then applied to a case study concerning an autonomous delivery vehicle service network design in Yuhang, China. Computational results validate the effectiveness of our optimization approach.

Keywords: intracity express delivery; service network design; support vector clustering-based data-driven; two-stage adjustable robust model; Benders dual decomposition
Mathematics Subject Classification: 90B06, 90C17

1. Introduction

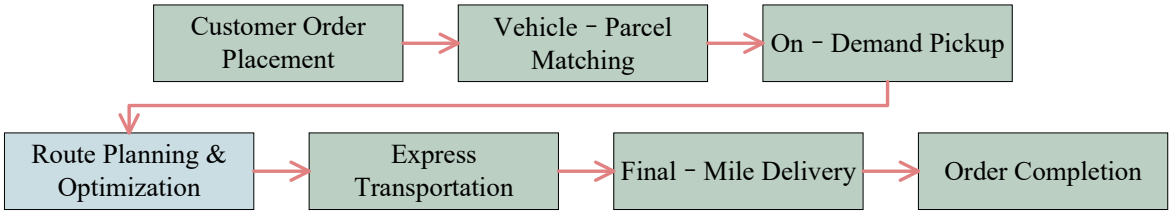

Figure 1. Flowchart of express delivery process.

Intracity express delivery refers to courier services operating within the same city or specific region, typically requiring completion of package collection, sorting, transportation, and delivery within a relatively short timeframe, such as next-day, same-day, or even within hours [1], as shown in Figure 1. In recent years, the intracity express delivery industry has experienced explosive growth driven by e-commerce, instant delivery, fresh food distribution, and local life services and has become a core component of modern urban logistics systems [2, 3]. According to the 2024 Postal Industry Development Statistical Bulletin issued by the State Post Bureau, China's express delivery volume reached 175.08 billion packages in 2024, representing a year-on-year increase of 21.5%. Within this total, intracity express delivery accounted for 15.64 billion packages, growing by 14.6% year-on-year and constituting 8.9% of China's overall express delivery volume [4]. As illustrated in Figure 2, intracity express delivery has developed into a significant market segment within the courier industry.

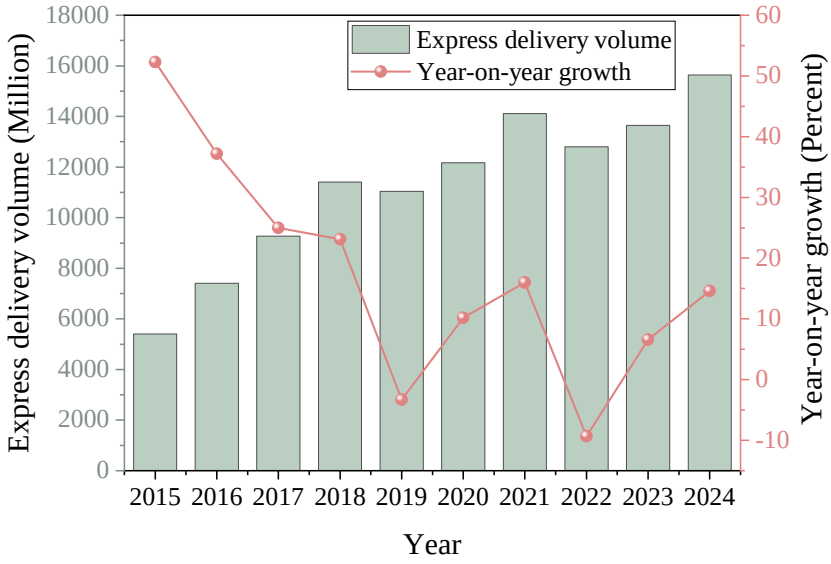

Figure 2. China's intracity express delivery business volume and growth rate from 2015 to 2024.

In practice, intracity express delivery operators face a persistent tension between stringent service commitments and uncertain demand [2, 5]. Unlike long-haul logistics systems with relatively longer lead times, intracity services are typically required to be completed within hours or the same day, and they operate with limited vehicle capacities under a fixed operational cycle [6]. Under such tight time windows and capacity constraints, demand deviations cannot be fully absorbed by minor

schedule adjustments. When demand surges within a narrow time interval, the preplanned network may experience capacity violations, missed deadlines, or unplanned outsourcing [7], which makes demand uncertainty a primary driver of feasibility and cost in service network design.

The demand volatility in intracity express delivery is induced by multiple operational factors. For example, promotion-driven events such as e-commerce campaigns, flash sales, and live-streaming sales can generate abrupt order bursts concentrated in short time periods, and seasonal and calendar-related patterns (e.g., holidays and weekends) shift both the demand level and its temporal distribution [8, 9]. Existing modeling paradigms have limitations to address this setting. Deterministic optimization relies on point forecasts and treats demands as known, which can yield capacity and routing decisions that become infeasible under realized deviations, thereby triggering costly ad-hoc interventions such as emergency dispatching or excessive outsourcing [10–12]. Stochastic optimization requires either a known probability distribution or scenario probabilities, which are often unavailable or difficult to justify in practice when demand distributions are uncertain and time-varying. These issues motivate a distribution-free robust modeling approach that can provide feasibility guarantees under uncertain demand while controlling conservatism.

To address these challenges, this study develops a new data-driven adjustable robust optimization (ARO) framework for intracity express delivery service network design. The framework constructs an uncertainty set from historical demand data and optimizes the service network with recourse actions to maintain feasibility under capacity and time-window constraints, where the robustness level can be calibrated by a regularization parameter.

The contributions of this study are characterized by four key aspects:

- We propose a two-stage optimization framework for intracity express delivery network design that minimizes total operational costs while simultaneously addressing routing, scheduling, and uncertain demand challenges.
- We develop a novel data-driven uncertainty set construction method based on a support vector clustering (SVC) technique that effectively leverages historical data to characterize demand uncertainty.
- We formulate an ARO model using the constructed uncertainty set, initially as a semi-infinite programming model, and then reformulate it into a robust counterpart through linear decision rules and duality technologies.
- We validate our approach using a real-world case study of an unmanned delivery vehicle service network design in Yuhang, Zhejiang, demonstrating that our model's solutions offer both uncertainty immunity and reduced conservatism compared to other optimization methods.

The organization of the remaining sections is as follows. Section 2 provides a systematic review of the relevant literature. Section 3 develops a data-driven ARO model for intracity express delivery network design. Section 4 derives the robust counterpart of the model under the proposed data-driven uncertainty set. Section 5 customizes a solution algorithm tailored to the structural characteristics of the model. Section 6 conducts numerical experiments on a real-world case study and discusses the practical aspects of deploying our proposed data-driven ARO framework. Finally, Section 7 summarizes the findings and outlines directions for future research.

2. Literature review

This section systematically reviews the literature from two key areas: intracity express delivery and delivery network design under uncertainty. Based on this review, we identify research gaps in existing literature and establish the motivation for our study.

2.1. Intracity express delivery network design under uncertainty

In actual operations, the design of intracity express delivery service network faces numerous uncertainties, with demand uncertainty being one of the most prominent challenges. Research on networks design under uncertainty mainly covers the following aspects:

Meng et al. [13] developed a two-stage stochastic programming model for the procurement of transportation capacity in automotive multimodal transport networks under uncertain demand conditions and proved it using the sample average approximation algorithm. Khalifehzadeh et al. [14] designed a stochastic multiobjective model for multilevel supply chains and used opportunistic constraint methods to handle the uncertainties of demand and delivery lead times. Yin et al. [15] proposed a two-stage stochastic programming model in the design of fourth-party logistics networks, simultaneously considering both facility disruptions and demand uncertainties. Petrovic et al. [16] proposed the concept of fuzzy scenarios to capture the uncertain changes in customer demands and developed a fuzzy multiobjective optimization model by using language terms and fuzzy number modeling. Sun [17] used trapezoidal fuzzy numbers to represent uncertain demand and transportation capacity and combined the fuzzy expected value method and the fuzzy ranking method to handle fuzzy constraints. Guo and Chen [18] employed the fuzzy opportunity constraint method in the configuration of green closed-loop supply chains to address the uncertainties in market and recycled product quality. Xiang et al. [19] proposed a robust optimization method with a penalty constraint for service network design problems, introducing a robustness index to balance the target value and penalize violations. The numerical experiments of Wu et al. [2] show that considering random factors can effectively reduce operating costs, especially in the case of tight vehicle capacity and loose time windows. This discovery emphasizes the importance of integrating the uncertainty of requirements in network design.

Although some studies have begun to focus on the issue of demand uncertainty, most of them remain at the level of demand forecasting or adopt simplified stochastic models, failing to fully consider the complex interaction between demand uncertainty and the conservation of network traffic, which makes it difficult to cope with the ever-changing market environment for practical applications.

2.2. Current research status of intracity express delivery

intracity delivery, which refers to logistics services that transport goods from one point to another within urban areas, was conceptualized by Taniguchi et al. [20]. The rapid growth of the intracity express delivery sector in recent years has attracted considerable scholarly attention, with researchers investigating various dimensions of network optimization.

From a strategic planning perspective, facility location and network structure optimization have been the central research themes. Liu et al. [5] introduced an integrated approach, combining multiple centrality assessment and multicriteria decision-making methods to optimize ground express delivery networks, demonstrating that transitioning from three-level to two-level networks can significantly

reduce both costs and delivery times. Wu et al. [2] examined the capacitated hub location routing problem with time windows and stochastic demands, developing a multistage recourse model that addresses both long-term strategic decisions such as hub location and short-term operational decisions such as vehicle routing. Similarly, Nicholson et al. [21] studied the design of unmanned aerial vehicle transportation networks in urban areas, proposing a bi-objective mixed-integer programming model to balance demand satisfaction and risk mitigation. At the tactical and operational levels, researchers have focused on routing optimization and service network design. Satici and Dayarian [22] addressed tactical and operational planning through multicommodity service network design that maximizes consolidation opportunities and meets strict service guarantees. Sun [17] investigated the routing optimization problem for door-to-door transportation of hazardous goods, employing fuzzy soft-time windows to optimize last-mile distribution through roadrail multimodal transport hub radiation networks. In the emerging crowdsourcing delivery context, Wang et al. [23] proposed an online, deep, reinforcement learning-based order recommendation framework for rider-centered food delivery systems, and Behrendt et al. [24] studied courier scheduling problems on crowdsourcing delivery platforms.

These studies collectively emphasize the significance of network optimization in the intracity express delivery operations. However, these studies often lack a comprehensive consideration of the design of the intracity express delivery system service network, especially under the framework of robust optimization, when resource allocation, capacity limitations, and vehicle route planning are taken into account simultaneously. Therefore, integrating these factors and constructing a robust intracity express delivery service network through robust optimization methods holds significant research value.

3. Methodology

3.1. Problem statement

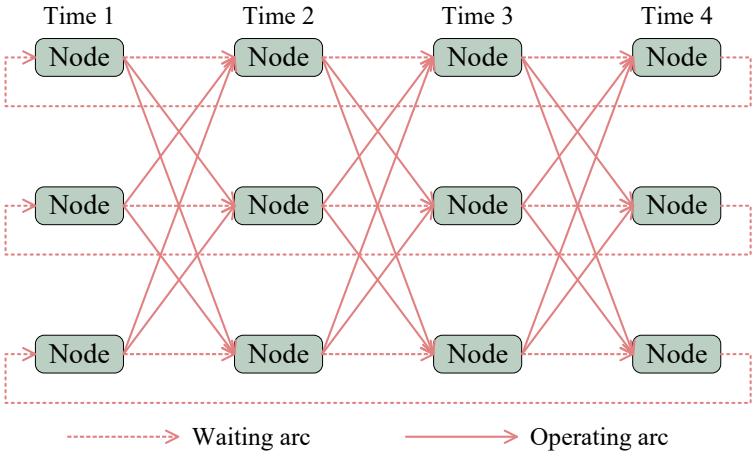

Figure 3. Time-space network for intracity express services.

This paper optimizes resource allocation and routing decisions in an intracity express delivery service network. This network operates on a discrete cyclic time horizon, where all commodities must be delivered within specific time windows. The cyclical nature of transportation operations is explicitly captured through a mathematical formulation that establishes seamless continuity between terminal

and initial periods, thereby creating a coherent operational cycle that reflects real-world logistics systems. The physical structure of the problem is mapped onto a time-space network, which comprises transportation arcs representing vehicle movements and waiting arcs representing nodal dwelling, as illustrated in Figure 3. All notations used throughout this paper are systematically defined as follows:

Sets:

$[I]$: Nodes set, index $i \in [I]$;
$[A]$: Arcs set, index $(i, i') \in [A]$;
$[C]$: Commodities set, index $c \in [C]$;
$[T]$: Time index set, index $t \in [T] = \{0, \ldots, T-1\}$;
$[\Xi]$: Scenario set, index $\xi \in [\Xi]$.

Parameters:

(O_c, D_c): Origin-destination pair for commodity c;
(γ_c, τ_c): Time window for shipping commodity c (γ_c: release time, τ_c: deadline);
$f_{ii'}$: Fixed cost for freight service on arc (i, i');
α: Outsourcing cost;
q: Vehicle capacity;
T: Length of cyclic time horizon (discrete periods);
$c_{ii'}$: Cost for freight service on arc (i, i');
t^-: Cyclic departure time, $t-1$, if $t \geq 1$; $T-1$, otherwise;
π^ξ: Probability of scenario ξ.

Uncertain parameter:

d_c^ξ: Demand of commodity c under scenario ξ.

Decision variables:

$X_{ii'}(t)$: Service frequency on arc (i, i') at time t;
$Y_{ii'c}^\xi(t)$: Flow of commodity c on arc (i, i') at time t under scenario ξ;
Z_c^ξ: Outsourcing volume for commodity c under scenario ξ.

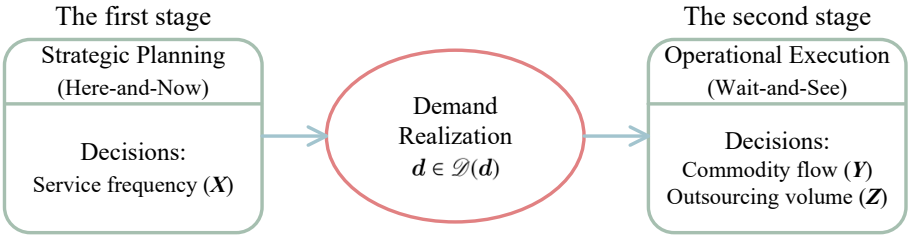

Figure 4. The decision process of the two-stage robust optimization.

We adopt a two-stage framework to reflect the structure of intracity express operations under uncertain demand. Figure 4 summarizes the decision timeline. In the first stage (here-and-now), the model determines the service frequencies $X_{ii'}(t)$ within the time-space network prior to the realization of daily demand. Operationally, $X_{ii'}(t)$ specifies the planned dispatch schedule and baseline fleet allocation over discrete periods, and it determines the available arc capacity $qX_{ii'}(t)$. After demand is realized, the second stage (wait-and-see) decides commodity flow allocations $Y_{ii'c}^\xi(t)$ and outsourcing volumes Z_c^ξ to route parcels through the planned services while satisfying time-window constraints. This separation improves realism relative to integrated formulations in which parcel flows are fixed jointly with service

decisions before observing demand. Fixing Y prior to demand realization would impose rigid flow plans that cannot adapt to demand fluctuations.

It is important to recognize that real-world logistics systems rarely operate under conditions of perfect information. Demands are typically characterized by uncertainty stemming from various sources, including market volatility, seasonal variations, and operational disruptions. The existence of this uncertainty may lead to the initial optimal decision being suboptimal. To enhance the robustness of our optimization framework, we proceed in the subsequent section to construct a SVC-based uncertainty set $\mathscr{D}(\boldsymbol{d})$ that characterizes the uncertain demands.

3.2. Uncertain set construction

The SVC employs kernel functions to project data points from the original space into a high-dimensional feature space. Within this feature space, the core objective of the SVC is to determine the minimal-volume hypersphere containing the mapped projections. When inversely mapped to the original space, this hypersphere forms contours encapsulating data clusters [25]. Fundamentally, SVC constructs minimal-volume closed hyperspheres encompassing all or dominant data points. The subsequent section details the data-driven uncertainty set formulation methodology based on this SVC framework.

Let $\mathcal{S} = \{\boldsymbol{d}^{(n)}\}_{n=1}^{N}$ denote a dataset of N sample demand vectors $\boldsymbol{d}$. Based on $\mathcal{S}$, SVC constructs a minimum-volume closed hypersphere that encloses the observations. The optimization model is formulated as

$$\min_{\boldsymbol{P},R} \; R^2 \quad \text{s.t.} \; \left\|\varphi\left(\boldsymbol{d}^{(n)}\right) - \boldsymbol{P}\right\|^2 \le R^2 \quad \forall n \in [N], \tag{3.1}$$

where R denotes the hypersphere radius, $\boldsymbol{P}$ represents its center, $\varphi(\cdot)$ is a nonlinear mapping from S to a reproducing kernel Hilbert space, and $\|\cdot\|$ is the Euclidean norm. To accommodate potential outliers and mitigate excessive radius expansion, we introduce nonnegative slack variables $\bar{\boldsymbol{\omega}} \in \mathbb{R}_+^N$ to transform the hard constraints of model (3.1) into their soft counterparts. In this formulation, $\bar{\omega}_n$ quantifies the deviation distance of the nth sample from the hypersphere boundary and functions as a penalty term within the objective function

$$\min_{\boldsymbol{P},R,\bar{\omega}} \; R^2 + \frac{1}{N\vartheta}\sum_{n\in[N]} \bar{\omega}_n \tag{3.2a}$$

$$\text{s.t.} \quad \|\varphi(\boldsymbol{d}^{(n)} - \boldsymbol{P})\|^2 \le R^2 + \bar{\omega}_n \quad \forall n \in [N], \tag{3.2b}$$

$$\bar{\omega}_n \ge 0 \quad \forall n \in [N], \tag{3.2c}$$

where $\vartheta > 0$ is a regularization parameter balancing hypersphere volume and constraint violations. We introduce the Lagrange multipliers $\boldsymbol{\beta} \in \mathbb{R}_+^N$ and $\boldsymbol{\lambda} \in \mathbb{R}_+^N$. Specifically, β_n denotes the dual variable associated with constraint (3.2b), whereas λ_n is assigned to constraint (3.2c). Accordingly, the Lagrangian function is formulated as follows:

$$\mathcal{L}(\boldsymbol{P}, R, \bar{\boldsymbol{\omega}}, \boldsymbol{\beta}, \boldsymbol{\lambda}) = R^2 + \frac{1}{N\vartheta}\sum_{n\in[N]} \bar{\omega}_n - \sum_{n\in[N]} \beta_n \left(R^2 + \bar{\omega}_n - \left\|\varphi(\boldsymbol{d}^{(n)}) - \boldsymbol{P}\right\|^2\right) - \sum_{n\in[N]} \lambda_n \bar{\omega}_n.$$

The first-order optimality conditions yield

$$\begin{cases} \sum\limits_{n\in[N]} \beta_n = 1, \\ \boldsymbol{P} = \sum\limits_{n\in[N]} \beta_n \varphi(\boldsymbol{d}^{(n)}), \\ \beta_n + \lambda_n = \dfrac{1}{N\vartheta}. \end{cases}$$

Subsequently, the dual problem of model (3.2) is formulated as follows:

$$\begin{aligned} \min_{\boldsymbol{\beta}} \quad & \sum_{n\in[N]} \sum_{n'\in[N]} \beta_n \beta_{n'} K(\boldsymbol{d}^{(n)}, \boldsymbol{d}^{(n')}) - \sum_{n\in[N]} \beta_n K(\boldsymbol{d}^{(n)}, \boldsymbol{d}^{(n)}) \\ \text{s.t.} \quad & 0 \le \beta_n \le \frac{1}{N\vartheta}, \quad \forall n \in [N], \\ & \sum_{n\in[N]} \beta_n = 1, \end{aligned} \tag{3.3}$$

where $K(\boldsymbol{d}^{(n)}, \boldsymbol{d}^{(n')}) = \varphi(\boldsymbol{d}^{(n)})^T \varphi(\boldsymbol{d}^{(n')})$ is the kernel function, and the complementary slackness conditions are given by

$$\begin{aligned} &\lambda_n \bar{\omega}_n = 0, \\ &\beta_n \left(R^2 + \bar{\omega}_n - \left\| \varphi(\boldsymbol{d}^{(n)}) - \boldsymbol{P} \right\|^2 \right) = 0. \end{aligned}$$

In summary, we have the following:

If $\boldsymbol{d}^{(n)}$ is inside the sphere, that is, $\left\| \varphi(\boldsymbol{d}^{(n)}) - \boldsymbol{P} \right\|^2 < R^2 \implies \beta_n = 0, \lambda_n = \dfrac{1}{N\vartheta}$,

If $\boldsymbol{d}^{(n)}$ is on the boundary of the sphere, that is, $\left\| \varphi(\boldsymbol{d}^{(n)}) - \boldsymbol{P} \right\|^2 = R^2 \implies 0 < \beta_n < \dfrac{1}{N\vartheta}$,

If $\boldsymbol{d}^{(n)}$ is outside the sphere, that is, $\left\| \varphi(\boldsymbol{d}^{(n)}) - \boldsymbol{P} \right\|^2 > R^2 \implies \beta_n = \dfrac{1}{N\vartheta},\ \gamma_n = 0$.

We define the support vector index set as $\mathscr{O} = \{n \mid \beta_n > 0\}$ and the boundary support vector index set as $\mathscr{B} = \{n \mid 0 < \beta_n < \frac{1}{N\vartheta}\}$. The radius R equates to the distance from center $\boldsymbol{P}$ to any $\mathbf{d}^{(n')}$ ($n' \in \mathscr{B}$):

$$\begin{aligned} R^2 &= \left\| \varphi(\boldsymbol{d}^{(n')}) - \boldsymbol{P} \right\|^2 \\ &= K(\boldsymbol{d}^{(n')}, \boldsymbol{d}^{(n')}) - 2 \sum_{n=1}^{N} \beta_n K(\boldsymbol{d}^{(n')}, \boldsymbol{d}^{(n)}) \\ &\quad + \sum_{n,m=1}^{N} \beta_n \beta_m K(\boldsymbol{d}^{(n)}, \boldsymbol{d}^{(m)}), \quad n' \in \mathscr{B}. \end{aligned} \tag{3.4}$$

Therefore, the uncertainty set of uncertain demand $\boldsymbol{d}$ can be described as

$$\mathscr{D}(\boldsymbol{d}) = \left\{ \boldsymbol{d} \middle| K(\boldsymbol{d}, \boldsymbol{d}) - 2 \sum_{n=1}^{N} \beta_n K(\boldsymbol{d}, \boldsymbol{d}^{(n)}) + \sum_{n,m=1}^{N} \beta_n \beta_m K(\boldsymbol{d}^{(n)}, \boldsymbol{d}^{(m)}) \le R^2 \right\}. \tag{3.5}$$

This paper adopts the weighted generalized intersection kernel proposed by Shang et al. [26], in which

$$K(\boldsymbol{d}^{(n')}, \boldsymbol{d}^{(n)}) = \sum_{m=1}^{n} h_m - \left\| \overline{\boldsymbol{W}} (\boldsymbol{d}^{(n')} - \boldsymbol{d}^{(n)}) \right\|_1, \tag{3.6}$$

where $\overline{\boldsymbol{W}} = \Sigma^{-1/2}$ is the weighting matrix (Σ denotes the unbiased covariance matrix of $\{\boldsymbol{d}^{(n)}\}_{n=1}^{N}$), and $h_m > \max_n \bar{\boldsymbol{w}}_m^\top \boldsymbol{d}^{(n)} - \min_n \bar{\boldsymbol{w}}_m^\top \boldsymbol{d}^{(n)}$ ($\bar{\boldsymbol{w}}_m$: m-th column of $\overline{\boldsymbol{W}}$). In conclusion, the uncertainty set (3.5) can be equivalently described as

$$\mathscr{D}(\boldsymbol{d}) = \left\{ \boldsymbol{d} \middle| \sum_{n\in\mathscr{O}} \beta_n \left\| \overline{\boldsymbol{W}}(\boldsymbol{d} - \boldsymbol{d}^{(n)}) \right\|_1 \le \sum_{n\in\mathscr{O}} \beta_n \left\| \overline{\boldsymbol{W}}(\boldsymbol{d}^{(n')} - \boldsymbol{d}^{(n)}) \right\|_1 \quad \forall n' \in \mathscr{B} \right\}, \tag{3.7}$$

which is provably convex.

Algorithm 1 details the Python implementation for constructing the data-driven uncertainty set (3.7).

Algorithm 1: Uncertainty set construction algorithm

Input: Dataset $\mathcal{S}$

Output: Data-driven uncertainty set $\mathscr{D}(\boldsymbol{d})$

Phase 1: Kernel Function Computation

Compute weighting matrix $\overline{\boldsymbol{W}}$;

Determine optimal parameter values h_m based on $\overline{\boldsymbol{W}}$;

Generate kernel matrix $\boldsymbol{K} = \{K(\boldsymbol{d}^{(n')}, \boldsymbol{d}^{(n)})\}$ by integrating $\overline{\boldsymbol{W}}$, h_m, and $\mathcal{S}$ into Eq. (3.6).

Phase 2: Support Vector Identification

Optimize model (3.3) with kernel matrix $\boldsymbol{K}$ to obtain coefficient vector $\boldsymbol{\beta}$;

Form support vector and boundary support vector index sets.

Phase 3: Uncertainty Set Formulation

Evaluate radius R utilizing Eq. (3.4);

Formulate the explicit representation of uncertainty set $\mathscr{D}(\boldsymbol{d})$ as in Eq. (3.7) by incorporating $\boldsymbol{K}$ and R into Eq. (3.5).

return Data-driven uncertainty set $\mathscr{D}(\boldsymbol{d})$

Remark 3.1. The weighted generalized intersection kernel meets the tractability requirements of our proposed data-driven ARO framework. As noted by Shang et al. [26], kernels such as the radial basis function kernel introduces nonlinearities that hinder a tractable linear robust counterpart, whereas the adopted kernel preserves a linearizable set representation and supports an equivalent mixed-integer linear programming reformulation. Regarding the selection of SVC parameters: (i) $\vartheta \in (0, 1)$ controls the outlier fraction via $0 \le \beta_n \le 1/(N\vartheta)$ in (3.3), where a smaller ϑ yields a larger set, and a larger ϑ yields a smaller set; in practice, ϑ is aligned with the target coverage $1 - \vartheta$ and can be checked by empirical holdout coverage. (ii) $\overline{\boldsymbol{W}} = \Sigma^{-1/2}$ is computed from the unbiased covariance matrix of historical samples, standardizing demand dimensions without additional tuning. (iii) $\{h_m\}$ are computed from data ranges to satisfy the condition of (3.6), and thus are not tuned via extensive search.

Remark 3.2. We adopt SVC to construct the demand uncertainty set in a data-driven and distribution-free manner, which is appropriate for intracity express delivery where the demand distribution is not known a priori and parametric assumptions or scenario probabilities are difficult to evaluate exactly. Embedding the resulting set $\mathscr{D}(\boldsymbol{d})$ into the ARO model yields adjustable recourse decisions that remain feasible for all $\boldsymbol{d} \in \mathscr{D}(\boldsymbol{d})$. In contrast, the classical budgeted uncertainty set defined in Appendix B is specified through componentwise bounds and a budget parameter and do not provide an explicit data-calibrated coverage guarantee. Consequently, it may include demand realizations that are weakly supported by historical observations, as illustrated in Figure 5, which increases conservatism and can lead to higher capacity provisioning in worst-case designs.

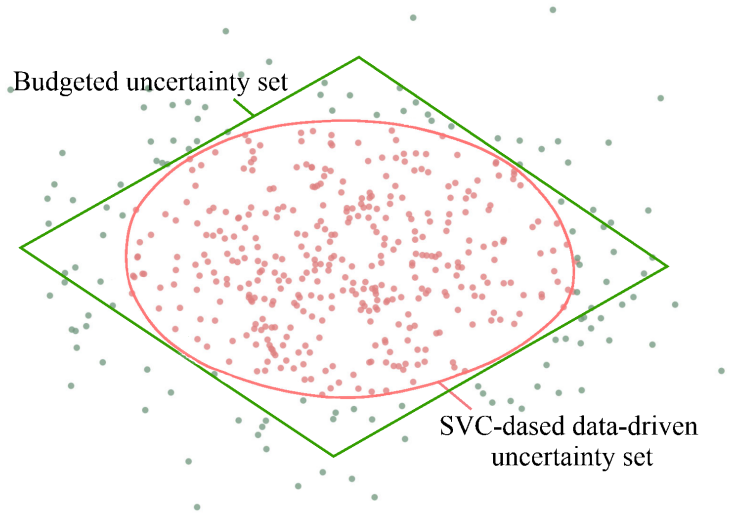

Figure 5. Comparison between budgeted and SVC-based data-driven uncertainty sets.

As the basis for subsequent robust optimization, this uncertainty set enables the construction of a data-driven ARO decision-making framework in Section 3.3 that preserves operational efficiency under uncertain demands.

3.3. Data-driven ARO model formulation for intracity express delivery problem

Leveraging constructed uncertainty set (3.7) with the SVC technique, we formulate the following data-driven ARO framework for the intracity express delivery service network design problem under uncertainty.

Our two-stage model is established as follows.

First stage: This stage determines strategic service frequencies, minimizing the sum of fixed costs and expected recourse costs.

$$\min_{\boldsymbol{X}} \sum_{(i,i')\in[A]} \sum_{t\in[T]} f_{ii'} X_{ii'}(t) + \alpha \sum_{\xi\in[\Xi]} \pi^{\xi} R(\boldsymbol{X}, \boldsymbol{d}^{\xi}) \tag{3.8a}$$

$$\text{s.t.} \sum_{i'\in[I]} X_{i'i}(t^{-}) - \sum_{i'\in[I]} X_{ii'}(t) = 0 \quad \forall i \in [I],\ \forall t \in [T], \tag{3.8b}$$

$$X_{ii'}(t) \in \mathbb{Z}^{+} \quad \forall (i,i') \in [A],\ \forall t \in [T]. \tag{3.8c}$$

Objective function (3.8a) contains two cost components: the fixed costs associated with establishing service frequencies on network arcs and the expected recourse cost that captures the consequences of strategic decisions under various scenarios. These expected recourse costs are weighted by scenario probabilities and outsourcing cost.

Constraints (3.8b) enforce vehicle flow conservation at each node across the cyclic time horizon, ensuring operational continuity by establishing that the number of vehicles arriving at each node equals the number departing. This constraint maintains the cyclical integrity of the service schedule. Constraints (3.8c) restrict service frequencies to nonnegative integers, reflecting the discrete nature of vehicle deployment decisions.

Second stage: This stage determines operational decisions concerning commodity flow routing and outsourcing quantities to fulfill demand under a specific scenario. The second-stage objective function minimizes the total outsourcing volume across all commodities, accounting for the recourse actions required when the established network capacity is insufficient:

$$R(\boldsymbol{X}, \boldsymbol{d}^{\xi}) = \min_{\boldsymbol{Y},\boldsymbol{Z}} \sum_{c\in[C]} Z_c^{\xi} \tag{3.8d}$$

$$\text{s.t.} \sum_{c\in[C]} Y_{ii'c}^{\xi}(t) \le q \cdot X_{ii'}(t) \quad \forall (i,i') \in [A],\ i \ne i',\ \forall t \in [T], \tag{3.8e}$$

$$\sum_{i'\in[I]} Y_{O_c i' c}^{\xi}(\gamma_c) - \sum_{i'\in[I]} Y_{i' O_c c}^{\xi}(\gamma_c) = d_c^{\xi} - Z_c^{\xi} \quad \forall \boldsymbol{d} \in \mathscr{D}(\boldsymbol{d}),\ \forall c \in [C], \tag{3.8f}$$

$$\sum_{i'\in[I]} Y_{D_c i' c}^{\xi}(\tau_c) - \sum_{i'\in[I]} Y_{i' D_c c}^{\xi}(\tau_c) = -d_c^{\xi} + Z_c^{\xi} \quad \forall \boldsymbol{d} \in \mathscr{D}(\boldsymbol{d}),\ \forall c \in [C], \tag{3.8g}$$

$$\sum_{i'\in[I]} Y_{ii'c}^{\xi}(t) - \sum_{i'\in[I]} Y_{i'ic}^{\xi}(t) = 0$$

$$\forall i \in [I],\ \forall t \in [T],\ (i \ne O_c, t \ne \gamma_c) \wedge (i \ne D_c, t \ne \tau_c),\ \forall c \in [C], \tag{3.8h}$$

$$Y_{ii'c}^{\xi}(\tau_c) = 0 \quad \forall (i,i') \in [A],\ \forall c \in [C], \tag{3.8i}$$

$$Z_c^{\xi} \ge 0 \quad \forall c \in [C], \tag{3.8j}$$

$$Y_{ii'c}^{\xi}(t) \ge 0 \quad \forall (i,i') \in [A],\ \forall c \in [C],\ \forall t \in [T]. \tag{3.8k}$$

Capacity constraints (3.8e) ensure that commodity flows on each arc do not exceed the available capacity, which is determined by the product of vehicle capacity and service frequency. Constraints (3.8f)–(3.8h) enforce flow conservation for each commodity at every node and time period, with specific conditions for origin nodes (where and when commodities enter the network) and destination nodes (where and when they exit). These constraints integrate outsourcing options, allowing demand to be fulfilled partially through the established network and partially via external services as needed. Notably, demand $\boldsymbol{d}$ is parameterized as an uncertain variable within the uncertainty set $\mathscr{D}(\boldsymbol{d})$. Constraints (3.8i) enforce time window requirements by prohibiting commodity flows beyond their specified deadlines, thereby ensuring strict adherence to delivery schedules. Finally, constraints (3.8j) and (3.8k) impose nonnegativity conditions on commodity flows and outsourcing variables to guarantee physical feasibility.

4. Model analysis

The proposed data-driven ARO model (3.8) involves semi-infinite constraints induced by the uncertainty set $\mathscr{D}(\boldsymbol{d})$, rendering the problem computationally intractable. To resolve this issue, we derive an equivalent robust counterpart through a framework comprising three phases: (i) structural analysis of the uncertainty set; (ii) application of linear decision rules to approximate adaptive recourse actions as affine functions of uncertain parameters; (iii) reformulation into an equivalent mixed-integer linear programming via duality theory, converting semi-infinite constraints into tractable inequalities.

4.1. Uncertainty set analysis

We define the parameter θ as

$$\theta = \min_{n' \in \mathscr{B}} \left\{ \sum_{n \in \mathscr{O}} \beta_n \left\| \overline{\boldsymbol{W}} (\boldsymbol{d}^{(n')} - \boldsymbol{d}^{(n)}) \right\|_1 \right\}$$

and introduce auxiliary vectors $\{\boldsymbol{\varrho}_n\}_{n \in \mathscr{O}}$. Uncertainty set (3.7) admits the equivalent representation:

$$\mathscr{D}(\boldsymbol{d}) = \left\{ \boldsymbol{d} \,\middle|\, \exists \boldsymbol{\varrho}_n \ \forall n \in \mathscr{O} : \begin{array}{l} \sum_{n \in \mathscr{O}} \beta_n \boldsymbol{\varrho}_n^\top \mathbf{1} \le \theta \\ -\boldsymbol{\varrho}_n \le \overline{\boldsymbol{W}} (\boldsymbol{d} - \boldsymbol{d}^{(n)}) \le \boldsymbol{\varrho}_n \ \ \forall n \in \mathscr{O} \end{array} \right\}, \tag{4.1}$$

where $\mathbf{1}$ denotes an all-ones vector.

For $0 \le \vartheta < 1$, the uncertainty set $\mathscr{D}(\boldsymbol{d})$ is nonempty and bounded, satisfying the asymptotic property

$$\lim_{N \to \infty} \mathbb{P} \left(\boldsymbol{d} \in \mathscr{D}(\boldsymbol{d}) \right) = 1 - \vartheta.$$

Thus, $\mathscr{D}(\boldsymbol{d})$ constitutes a $(1 - \vartheta)$-confidence region. In other words, the regularization parameter ϑ serves as an upper bound on the proportion of outliers. Consequently, the quantity of outliers can be controlled by tuning ϑ, which provides a data-driven mechanism to calibrate the conservatism of the uncertainty set.

4.2. Linear decision rule

In our setting, demand uncertainty enters the commodity flow-balance equalities. If all decisions were required to be nonadjustable, these equalities would need to hold simultaneously for every demand realization in the uncertainty set $\mathscr{D}(\boldsymbol{d})$. As shown by Ben-Tal et al. [27], incorporating uncertainty-affected equality constraints is structurally infeasible within the framework of static robust optimization. Therefore, a two-stage adjustable structure is necessary from a feasibility standpoint: The first stage fixes the service schedule and capacity provisioning, and the second stage allows the flow allocation and outsourcing decisions to adapt to the realized demand. The linear decision rule introduced below provides a tractable way to implement this adjustability, ensuring that the flow-balance equalities remain valid for all demands covered by uncertainty set $\mathscr{D}(\boldsymbol{d})$ [28].

Definition 4.1. The uncertain problem (3.8) is said to exhibit fixed recourse if the coefficients corresponding to all adjustable variables Z_c^ξ and $Y_{ii'c}^\xi(t)$ are certain; that is, the coefficient parameter α is independent of ξ.

Motivated by the fixed recourse property of model (3.8), we adopt affine decision rules to characterize the adaptive variables. As established by Ben-Tal et al. [27], this specific structure guarantees that the resulting adjustable robust counterpart remains computationally tractable.

Accordingly, we adopt the linear decision rule framework to address the second-stage decision-making process. Under this paradigm, recourse decisions are parameterized as affine functions of the random parameters, thereby establishing a linear mathematical relationship between the uncertain demands and the corresponding decision variables [29], as follows:

$$\begin{aligned} Z_c^\xi &= \bar{Z}_c^\xi + \sum_{c' \in [C]} \tilde{Z}_{cc'}^\xi d_{c'}^\xi \\ Y_{ii'c}^\xi(t) &= \bar{Y}_{ii'c}^\xi(t) + \sum_{c' \in [C]} \tilde{Y}_{ii'cc'}^\xi(t) d_{c'}^\xi. \end{aligned}$$

These equations explicitly characterize the recourse variables Z_c^ξ and $Y_{ii'c}^\xi(t)$ as affine functions of the uncertain demand. By substituting these functional relationships into model (3.8), we reformulate the original problem as follows:

$$\min_{\boldsymbol{X},\bar{\boldsymbol{Z}},\tilde{\boldsymbol{Z}},\bar{\boldsymbol{Y}},\tilde{\boldsymbol{Y}}} \quad \text{(3.8a)} \tag{4.2a}$$

$$\text{s.t.} \quad \text{constraints (3.8b), (3.8c),} \tag{4.2b}$$

$$R(\boldsymbol{X},\boldsymbol{d}^\xi) = \min\Big(\sum_{c\in[C]}\Big(\bar{Z}_c^\xi + \sum_{c'\in[C]}\tilde{Z}_{cc'}^\xi d_{c'}^\xi\Big)\Big)_{\forall \boldsymbol{d}\in\mathscr{D}(\boldsymbol{d})} \tag{4.2c}$$

$$\sum_{c\in[C]}\Big(\bar{Y}_{ii'c}^\xi(t) + \sum_{c'\in[C]}\tilde{Y}_{ii'cc'}^\xi(t)d_{c'}^\xi\Big) \le q\cdot X_{ii'}(t)$$

$$\forall \boldsymbol{d}\in\mathscr{D}(\boldsymbol{d}),\ \forall (i,i')\in[A],\ i\neq i',\forall t\in[T], \tag{4.2d}$$

$$\sum_{i'\in[I]}\Big(\bar{Y}_{O_ci'c}^\xi(\gamma_c) + \sum_{c'\in[C]}\tilde{Y}_{O_ci'cc'}^\xi(\gamma_c)d_{c'}^\xi\Big) - \sum_{i'\in[I]}\Big(\bar{Y}_{i'O_cc}^\xi(\gamma_c) + \sum_{c'\in[C]}\tilde{Y}_{i'O_ccc'}^\xi(\gamma_c)d_{c'}^\xi\Big)$$
$$= d_c^\xi - \Big(\bar{Z}_c^\xi + \sum_{c'\in[C]}\tilde{Z}_{cc'}^\xi d_{c'}^\xi\Big) \quad \forall \boldsymbol{d}\in\mathscr{D}(\boldsymbol{d}),\ \forall c\in[C], \tag{4.2e}$$

$$\sum_{i'\in[I]}\Big(\bar{Y}_{D_ci'c}^\xi(\tau_c) + \sum_{c'\in[C]}\tilde{Y}_{D_ci'cc'}^\xi(\tau_c)d_{c'}^\xi\Big) - \sum_{i'\in[I]}\Big(\bar{Y}_{i'D_cc}^\xi(\tau_c) + \sum_{c'\in[C]}\tilde{Y}_{i'D_ccc'}^\xi(\tau_c)d_{c'}^\xi\Big)$$
$$= -d_c^\xi + \Big(\bar{Z}_c^\xi + \sum_{c'\in[C]}\tilde{Z}_{cc'}^\xi d_{c'}^\xi\Big) \quad \forall \boldsymbol{d}\in\mathscr{D}(\boldsymbol{d}),\ \forall c\in[C], \tag{4.2f}$$

$$\sum_{i'\in[I]}\Big(\bar{Y}_{ii'c}^\xi(t) + \sum_{c'\in[C]}\tilde{Y}_{ii'cc'}^\xi(t)d_{c'}^\xi\Big) - \sum_{i'\in[I]}\Big(\bar{Y}_{i'ic}^\xi(t) + \sum_{c'\in[C]}\tilde{Y}_{i'icc'}^\xi(t)d_{c'}^\xi\Big)$$
$$= 0\ \forall \boldsymbol{d}\in\mathscr{D}(\boldsymbol{d}),\forall i\in[I],\forall t\in[T],(i\neq O_c,t\neq\gamma_c)\wedge(i\neq D_c,t\neq\tau_c),\forall c\in[C], \tag{4.2g}$$

$$\bar{Y}_{ii'c}^\xi(\tau_c) + \sum_{c'\in[C]}\tilde{Y}_{ii'cc'}^\xi(\tau_c)d_{c'}^\xi = 0, \quad \forall \boldsymbol{d}\in\mathscr{D}(\boldsymbol{d}),\ \forall (i,i')\in[A],\ \forall c\in[C], \tag{4.2h}$$

$$\bar{Z}_c^\xi + \sum_{c'\in[C]}\tilde{Z}_{cc'}^\xi d_{c'}^\xi \ge 0 \quad \forall \boldsymbol{d}\in\mathscr{D}(\boldsymbol{d}),\ \forall c\in[C], \tag{4.2i}$$

$$\bar{Y}_{ii'c}^\xi(t) + \sum_{c'\in[C]}\tilde{Y}_{ii'cc'}^\xi(t)d_{c'}^\xi \ge 0 \quad \forall \boldsymbol{d}\in\mathscr{D}(\boldsymbol{d}),\ \forall (i,i')\in[A],\ \forall c\in[C],\ \forall t\in[T]. \tag{4.2j}$$

In summary, having analyzed the SVC-based uncertainty set and integrated the linear decision rule framework, we have established the theoretical structure of our proposed methodology. The main challenge lies in reformulating model (4.2) into a tractable robust counterpart. The subsequent section addresses this computational issue.

4.3. Tractable reformulation

This section reformulates the semi-infinite constraints in model (4.2).

Under the worst-case criterion, the right-hand side of constraint (4.2c) is rewritten as follows:

$$\min\Big(\sum_{c\in[C]}\bar{Z}_c^\xi + \sum_{c'\in[C]}\tilde{Z}_{cc'}^\xi d_{c'}^\xi\Big)_{\forall \boldsymbol{d}\in\mathscr{D}(\boldsymbol{d})} = \min\sum_{c\in[C]}\bar{Z}_c^\xi + \max_{\boldsymbol{d}\in\mathscr{D}(\boldsymbol{d})}\sum_{c'\in[C]}\tilde{Z}_{cc'}^\xi d_{c'}^\xi.$$

The derivation of a tractable counterpart, which leverages the structural properties of uncertainty set (3.7), is formalized in the following theorem.

Theorem 4.2. *Constraint* (4.2c) *can be reformulated as the following equivalent system within the interval* $0 < \theta < 1$*:*

$$R(\boldsymbol{X}, \boldsymbol{d}^{\xi}) = \min \sum_{c\in[C]} \Big(\bar{Z}_c^{\xi} + \sum_{n\in\mathscr{O}} (\dot{\boldsymbol{\Gamma}}_n^{c\xi} - \dot{\boldsymbol{\Lambda}}_n^{c\xi})^T \overline{\boldsymbol{W}} \boldsymbol{d}^{(n)} + \dot{\Omega}^{c\xi}\theta\Big) \tag{4.3a}$$

$$\text{s.t.} \sum_{n\in\mathscr{O}} \overline{\boldsymbol{W}}(\dot{\boldsymbol{\Lambda}}_n^{c\xi} - \dot{\boldsymbol{\Gamma}}_n^{c\xi}) + \tilde{\boldsymbol{Z}}_c^{\xi} = \boldsymbol{0}, \tag{4.3b}$$

$$\dot{\boldsymbol{\Lambda}}_n^{c\xi} + \dot{\boldsymbol{\Gamma}}_n^{c\xi} = \dot{\Omega}^{c\xi}\beta_n \boldsymbol{1} \quad \forall n \in \mathscr{O}, \tag{4.3c}$$

$$\dot{\boldsymbol{\Lambda}}_n^{c\xi}, \dot{\boldsymbol{\Gamma}}_n^{c\xi} \in R_+^{|C|},\ \dot{\Omega}^{c\xi} \in R_+ \quad \forall n \in \mathscr{O}. \tag{4.3d}$$

Proof. The proof is provided in Appendix A.1. □

Analogously, Theorems 4.3–4.5 establish the equivalent reformulations of constraints (4.2d), (4.2i), and (4.2j), respectively.

Theorem 4.3. *Constraints* (4.2d) *can be reformulated as the following equivalent system within the interval* $0 < \theta < 1$*:*

$$\sum_{c\in[C]} \bar{Y}_{ii'c}^{\xi}(t) + \sum_{c\in[C]} \Big(\sum_{n\in\mathscr{O}} (\ddot{\boldsymbol{\Gamma}}_n^{c\xi ii' t} - \ddot{\boldsymbol{\Lambda}}_n^{c\xi ii' t})^T \overline{\boldsymbol{W}} \boldsymbol{d}^{(n)} + \ddot{\Omega}^{c\xi ii' t}\theta\Big) \le q \cdot X_{ii'}(t)$$

$$\forall (i,i') \in [A],\ i \neq i', \forall t \in [T], \tag{4.4a}$$

$$\sum_{n\in\mathscr{O}} \overline{\boldsymbol{W}}(\ddot{\boldsymbol{\Lambda}}_n^{c\xi ii' t} - \ddot{\boldsymbol{\Gamma}}_n^{c\xi ii' t}) + \tilde{\boldsymbol{Y}}_{ii'c}^{\xi}(t) = \boldsymbol{0} \quad \forall (i,i') \in [A],\ i \neq i', \forall t \in [T], \tag{4.4b}$$

$$\ddot{\boldsymbol{\Lambda}}_n^{c\xi ii' t} + \ddot{\boldsymbol{\Gamma}}_n^{c\xi ii' t} = \ddot{\Omega}^{c\xi ii' t}\beta_n \boldsymbol{1} \quad \forall n \in \mathscr{O},\ \forall (i,i') \in [A],\ i \neq i', \forall t \in [T], \tag{4.4c}$$

$$\ddot{\boldsymbol{\Lambda}}_n^{c\xi ii' t}, \ddot{\boldsymbol{\Gamma}}_n^{c\xi ii' t} \in R_+^{|C|},\ \ddot{\Omega}^{c\xi ii' t} \in R_+ \quad \forall n \in \mathscr{O},\ \forall (i,i') \in [A],\ i \neq i', \forall t \in [T]. \tag{4.4d}$$

Proof. The proof is provided in Appendix A.2. □

Theorem 4.4. *Constraints* (4.2i) *can be reformulated as the following equivalent system within the interval* $0 < \theta < 1$*:*

$$\bar{Z}_c^{\xi} + \sum_{n\in\mathscr{O}} (\bar{\boldsymbol{\Gamma}}_n^{c\xi} - \bar{\boldsymbol{\Lambda}}_n^{c\xi})^T \overline{\boldsymbol{W}} \boldsymbol{d}^{(n)} + \bar{\Omega}^{c\xi}\theta \ge 0 \quad \forall c \in [C], \tag{4.5a}$$

$$\sum_{n\in\mathscr{O}} \overline{\boldsymbol{W}}(\bar{\boldsymbol{\Lambda}}_n^{c\xi} - \bar{\boldsymbol{\Gamma}}_n^{c\xi}) + \tilde{\boldsymbol{Z}}_c^{\xi} = \boldsymbol{0} \quad \forall c \in [C], \tag{4.5b}$$

$$\bar{\boldsymbol{\Lambda}}_n^{c\xi} + \bar{\boldsymbol{\Gamma}}_n^{c\xi} = \bar{\Omega}^{c\xi}\beta_n \boldsymbol{1} \quad \forall n \in \mathscr{O},\ \forall c \in [C], \tag{4.5c}$$

$$\bar{\boldsymbol{\Lambda}}_n^{c\xi}, \bar{\boldsymbol{\Gamma}}_n^{c\xi} \in R_-^{|C|},\ \dot{\Omega^c}\xi \in R_- \quad \forall n \in \mathscr{O},\ \forall c \in [C]. \tag{4.5d}$$

Proof. The proof is provided in Appendix A.3. □

Theorem 4.5. *Constraints* (4.2j) *can be reformulated as the following equivalent system within the interval* $0 < \theta < 1$*:*

$$\bar{Y}_{ii'c}^{\xi}(t) + \sum_{n\in\mathscr{O}} (\tilde{\boldsymbol{\Gamma}}_n^{c\xi ii' t} - \tilde{\boldsymbol{\Lambda}}_n^{c\xi ii' t})^T \overline{\boldsymbol{W}} \boldsymbol{d}^{(n)} + \tilde{\Omega}^{c\xi}\theta \ge 0 \quad \forall (i,i') \in [A],\ \forall c \in [C],\ t \in [T], \tag{4.6a}$$

$$\sum_{n\in\mathscr{O}} \overline{\boldsymbol{W}}(\tilde{\boldsymbol{\Lambda}}_n^{c\xi ii't} - \tilde{\boldsymbol{\Gamma}}_n^{c\xi ii't}) + \tilde{Y}^{\xi}_{ii'cc'}(t) = \mathbf{0} \quad \forall (i,i') \in [A],\ \forall c \in [C],\ t \in [T], \tag{4.6b}$$

$$\tilde{\boldsymbol{\Lambda}}_n^{c\xi} + \tilde{\boldsymbol{\Gamma}}_n^{c\xi} = \tilde{\Omega}^{c\xi ii't}\beta_n \mathbf{1} \quad \forall n \in \mathscr{O},\ \forall (i,i') \in [A],\ \forall c \in [C],\ t \in [T], \tag{4.6c}$$

$$\tilde{\boldsymbol{\Lambda}}_n^{c\xi ii't}, \tilde{\boldsymbol{\Gamma}}_n^{c\xi ii't} \in R_-^{|C|},\ \tilde{\Omega}^{c\xi ii't} \in R_- \quad \forall n \in \mathscr{O},\ \forall (i,i') \in [A],\ \forall c \in [C],\ \forall t \in [T]. \tag{4.6d}$$

Proof. The proof is provided in Appendix A.4. □

Given that the uncertainty set $\mathscr{D}(\boldsymbol{d})$ constitutes a full-dimensional domain, there exist $C+1$ affinely independent vectors within $\mathscr{D}(\boldsymbol{d})$, denoted as $\boldsymbol{d}^1, \boldsymbol{d}^2, \ldots, \boldsymbol{d}^{C+1}$. Consequently, constraints (4.2e)–(4.2h) are reformulated as follows:

$$\sum_{i'\in[I]} \bar{Y}^{\xi}_{O_c i' c}(\gamma_c) - \sum_{i'\in[I]} \bar{Y}^{\xi}_{i' O_c c}(\gamma_c) = -\bar{Z}^{\xi}_c \quad \forall c \in [C], \tag{4.7a}$$

$$\sum_{i'\in[I]}\sum_{c'\in[C]} \tilde{Y}^{\xi}_{O_c i' cc'}(\gamma_c) - \sum_{i'\in[I]}\sum_{c'\in[C]} \tilde{Y}^{\xi}_{i' O_c cc'}(\gamma_c) = 1 - \sum_{c'\in[C]} \tilde{Z}^{\xi}_{cc'} \quad \forall c \in [C], \tag{4.7b}$$

$$\sum_{i'\in[I]} \bar{Y}^{\xi}_{D_c i' c}(\tau_c) - \sum_{i'\in[I]} \bar{Y}^{\xi}_{i' D_c c}(\tau_c) = \bar{Z}^{\xi}_c \quad \forall c \in [C], \tag{4.7c}$$

$$\sum_{i'\in[I]}\sum_{c'\in[C]} \tilde{Y}^{\xi}_{D_c i' cc'}(\tau_c) - \sum_{i'\in[I]}\sum_{c'\in[C]} \tilde{Y}^{\xi}_{i' D_c cc'}(\tau_c) = -1 + \sum_{c'\in[C]} \tilde{Z}^{\xi}_{cc'} \quad \forall c \in [C], \tag{4.7d}$$

$$\begin{aligned}&\sum_{i'\in[I]} \bar{Y}^{\xi}_{ii'c}(t) - \sum_{i'\in[I]} \bar{Y}^{\xi}_{i'ic}(t) = 0\\ &\forall i \in [I],\ \forall t \in [T],\ (i \neq O_c, t \neq \gamma_c) \wedge (i \neq D_c, t \neq \tau_c),\ \forall c \in [C],\end{aligned} \tag{4.7e}$$

$$\begin{aligned}&\sum_{i'\in[I]}\sum_{c'\in[C]} \tilde{Y}^{\xi}_{ii'cc'}(t) - \sum_{i'\in[I]} \tilde{Y}^{\xi}_{i'ic}(t) = 0\\ &\forall i \in [I],\ \forall t \in [T],\ (i \neq O_c, t \neq \gamma_c) \wedge (i \neq D_c, t \neq \tau_c),\ \forall c \in [C],\end{aligned} \tag{4.7f}$$

$$\bar{Y}^{\xi}_{ii'c}(\tau_c) = 0, \quad \forall (i,i') \in [A],\ \forall c \in [C], \tag{4.7g}$$

$$\sum_{c'\in[C]} \tilde{Y}^{\xi}_{ii'cc'}(\tau_c) = 0, \quad \forall (i,i') \in [A],\ \forall c \in [C]. \tag{4.7h}$$

In virtue of Theorems 4.2–4.5, our proposed model (4.2) can be equivalently reformulated as the following mixed-integer linear programming problem:

$$\begin{aligned}&\min_{\substack{\boldsymbol{X},\bar{\boldsymbol{Z}},\tilde{\boldsymbol{Z}},\bar{\boldsymbol{Y}},\tilde{\boldsymbol{Y}},\dot{\boldsymbol{\Gamma}},\dot{\boldsymbol{\Lambda}},\dot{\Omega},\\ \ddot{\boldsymbol{\Gamma}},\ddot{\boldsymbol{\Lambda}},\ddot{\Omega},\tilde{\boldsymbol{\Gamma}},\tilde{\boldsymbol{\Lambda}},\tilde{\Omega},\tilde{\boldsymbol{\Gamma}},\tilde{\boldsymbol{\Lambda}},\tilde{\Omega}}} && \text{(3.8a)}\\ &\text{s.t.} && \text{constraints (3.8b), (3.8c), (4.3a)–(4.3d), (4.4a)–(4.4d), (4.5a)–(4.5d),}\\ &&& \text{(4.6a)–(4.6d), (4.7a)–(4.7h).}\end{aligned} \tag{4.8}$$

5. Solution approach

The Benders decomposition algorithm addresses optimization problems characterized by mixed variables. This method partitions the original formulation into a master problem comprising the complicating variables and a subproblem containing the remaining continuous variables. The procedure operates via an iterative process in which the master problem and subproblem exchange information

until convergence is attained. This section presents the problem reformulation and introduces a cut generation mechanism to improve computational efficiency.

The Benders decomposition algorithm is employed to address the optimization of the intracity express delivery service network, partitioning model (4.8) into a master problem and a subproblem.

Master problem:

$$\min \sum_{(i,i')\in[A]} \sum_{t\in[T]} f_{ii'} X_{ii'}(t) + \psi \tag{5.1a}$$

$$\text{s.t. constraints (3.8b), (3.8c),} \tag{5.1b}$$

where ψ denotes an auxiliary variable assisting in the calculation of the lower bound of the original formulation. The master problem optimizes service frequency decisions $\boldsymbol{X}^{\star}$. Upon solving the master problem, the determined values of $\boldsymbol{X}$ are fixed in the subproblem, which is formulated as follows.

Subproblem:

$$\min \alpha \sum_{\xi\in[\Xi]} \pi^{\xi} \sum_{c\in[C]} \Big(\bar{Z}_c^{\xi} + \sum_{n\in\mathscr{O}} (\dot{\boldsymbol{I}}_n^{c\xi} - \dot{\boldsymbol{\Lambda}}_n^{c\xi})^T \overline{\boldsymbol{W}} \boldsymbol{d}^{(n)} + \dot{\Omega}^{c\xi}\theta\Big) \tag{5.2a}$$

$$\text{s.t.} \sum_{c\in[C]} \bar{Y}_{ii'c}^{\xi}(t) + \sum_{c\in[C]} \Big(\sum_{n\in\mathscr{O}} (\ddot{\boldsymbol{I}}_n^{c\xi ii't} - \ddot{\boldsymbol{\Lambda}}_n^{c\xi ii't})^T \overline{\boldsymbol{W}} \boldsymbol{d}^{(n)} + \ddot{\Omega}^{c\xi ii't}\theta\Big) \le q \cdot X_{ii'}^{\star}(t)$$

$$\forall (i,i') \in [A],\ i \neq i', \forall t \in [T], \tag{5.2b}$$

$$\text{constraints (4.3b)–(4.3d), (4.4b)–(4.4d), (4.5a)–(4.5d), (4.6a)–(4.6d), (4.7a)–(4.7h).} \tag{5.2c}$$

Upon solving the subproblem, the results are returned to the master problem to facilitate the iterative process. Owing to the property of relatively complete recourse, which ensures subproblem feasibility for any fixed master problem solution, the algorithm exclusively generates optimality cuts. Specifically, these cuts are constructed via duality theory using the dual information of the subproblems, as formulated below:

$$\sum_{(i,i')\in[A],\ i\neq i'} \sum_{t\in[T]} q \cdot X_{ii'}(t) \cdot \zeta_{ii'}^{dual}(t) \le \psi,$$

where $\boldsymbol{\zeta}^{\boldsymbol{dual}}$ is the vector of dual variables associated with constraint (5.2b).

The aforementioned formulation establishes the master-subproblem framework via the Benders decomposition algorithm. However, the standard approach typically exhibits slow convergence, necessitating a substantial number of iterations [30]. To mitigate the resulting computational burden, this section introduces a cut generation strategy based on Benders dual decomposition [31]. Within this framework, the subproblem incorporating the copied variable $\tilde{\boldsymbol{X}}$ is reformulated as follows:

$$\min \alpha \sum_{\xi\in[\Xi]} \pi^{\xi} \sum_{c\in[C]} \Big(\bar{Z}_c^{\xi} + \sum_{n\in\mathscr{O}} (\dot{\boldsymbol{I}}_n^{c\xi} - \dot{\boldsymbol{\Lambda}}_n^{c\xi})^T \overline{\boldsymbol{W}} \boldsymbol{d}^{(n)} + \dot{\Omega}^{c\xi}\theta\Big) \tag{5.3a}$$

$$\text{s.t.} \sum_{i'\in[I]} \tilde{X}_{i'i}(t^-) - \sum_{i'\in[I]} \tilde{X}_{ii'}(t) = 0 \quad \forall i \in [I],\ \forall t \in [T], \tag{5.3b}$$

$$\sum_{c\in[C]} \bar{Y}_{ii'c}^{\xi}(t) + \sum_{c\in[C]} \Big(\sum_{n\in\mathscr{O}} (\ddot{\boldsymbol{I}}_n^{c\xi ii't} - \ddot{\boldsymbol{\Lambda}}_n^{c\xi ii't})^T \overline{\boldsymbol{W}} \boldsymbol{d}^{(n)} + \ddot{\Omega}^{c\xi ii't}\theta\Big) \le q \cdot \tilde{X}_{ii'}(t)$$

$$\forall (i,i') \in [A],\ i \neq i', \forall t \in [T], \tag{5.3c}$$

$$\tilde{X}_{ii'}(t) = X_{ii'}^{\star}(t) \quad \forall (i,i') \in [A],\ \forall t \in [T], \tag{5.3d}$$

$$\tilde{X}_{ii'}(t) \geq 0 \quad \forall (i,i') \in [A],\ \forall t \in [T], \tag{5.3e}$$

$$\text{constraints (4.3b)–(4.3d), (4.4b)–(4.4d), (4.5a)–(4.5d), (4.6a)–(4.6d), (4.7a)–(4.7h).} \tag{5.3f}$$

Constraints (5.3b) are rendered redundant by constraints (5.3d). The latter incorporate the auxiliary variables $\tilde{\boldsymbol{X}}$, and constraint (5.3e) specifies their feasible domain. Within the dual framework, let $\boldsymbol{\zeta}$ denote the vector of dual multipliers associated with constraints (5.3d). These multipliers correspond to the decision variables of the dual subproblem. Given a feasible solution $\boldsymbol{X}^\star$, solving the reformulated subproblem model (5.3) yields the following optimality cut:

$$\alpha \sum_{\xi \in [\Xi]} \pi^\xi \sum_{c \in [C]} \Big(\bar{Z}_c^{\xi,\star} + \sum_{n \in \mathscr{O}} (\dot{\boldsymbol{\Gamma}}_n^{c\xi,\star} - \dot{\boldsymbol{\Lambda}}_n^{c\xi,\star})^T \overline{\boldsymbol{W}} \boldsymbol{d}^{(n)} + \dot{\Omega}^{c\xi,\star} \theta \Big) + \sum_{(i,i') \in [A]} \sum_{t \in [T]} \zeta_{ii'}^\star(t) \Big(X_{ii'}(t) - \tilde{X}_{ii'}^\star(t) \Big) \leq \psi,$$

where $(\bar{\boldsymbol{Z}}^\star, \dot{\boldsymbol{\Gamma}}^\star, \dot{\boldsymbol{\Lambda}}^\star, \dot{\boldsymbol{\Omega}}^\star, \tilde{\boldsymbol{X}}^\star)$ and $\boldsymbol{\zeta}$ denote the optimal solution to subproblem (5.3) and the dual multiplier vector associated with constraint (5.3d), respectively.

6. Case study

Section 6.1 validates the proposed method via a small-scale numerical example, facilitating an intuitive presentation of model results and performance analysis. Subsequently, Section 6.2 applies the SVC-based data-driven ARO framework to an autonomous delivery vehicle service network design problem in Yuhang, Zhejiang, China, followed by a sensitivity analysis of key parameters.

6.1. A numerical example

The numerical instance is adapted from Lium et al. [32], characterized by dimensions of $I = 6$ nodes, $T = 3$ periods, and $C = 3$ commodities. Transportation costs are fixed at 100 for $i = i'$ and drawn uniformly from the interval $[100, 250]$ for $i \neq i'$. The vehicle capacity is fixed at 20. Demand values follow a truncated normal distribution $N(9, 5)$ defined over the interval $[0, \mu + 2\sigma]$, and Table 1 summarizes the remaining parameters. This section conducts numerical experiments to compare the proposed data-driven ARO model against its nominal counterpart. Regarding notation, I_i denotes the ith node in the physical network.

Table 1. The relevant parameters in the example.

Set $[C]$	Parameter			
	O_c	D_c	γ_c	τ_c
C_1	1	6	2	3
C_2	2	6	1	3
C_3	1	6	2	3

Figure 6 depicts the solution yielded by the proposed data-driven ARO model. In this graphical representation, colored lines correspond to product delivery routes, and blue service bands represent

vehicle service legs, with the band width indicating the number of vehicles deployed. Based on this visual framework, the data-driven solution involves the deployment of two vehicles: the first vehicle originates at Node 2, traversing Nodes 1 and 6 prior to returning to Node 2, while the second vehicle departs from Node 6, visiting Node 1 and subsequently returning to Node 6. Under this routing configuration, the demands for all three commodities (C1, C2, and C3) are fulfilled within the specified time horizon.

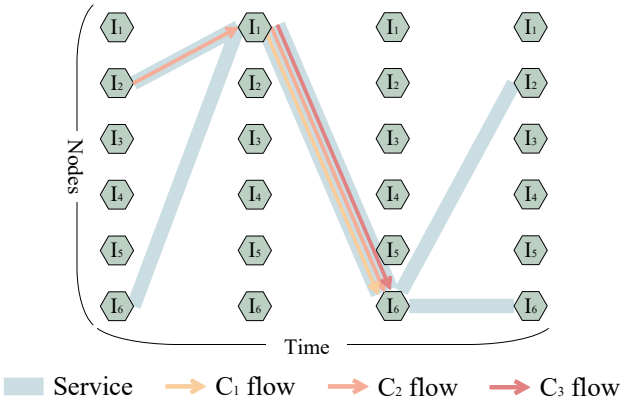

Figure 6. Optimal network design configuration yielded by the data-driven ARO model.

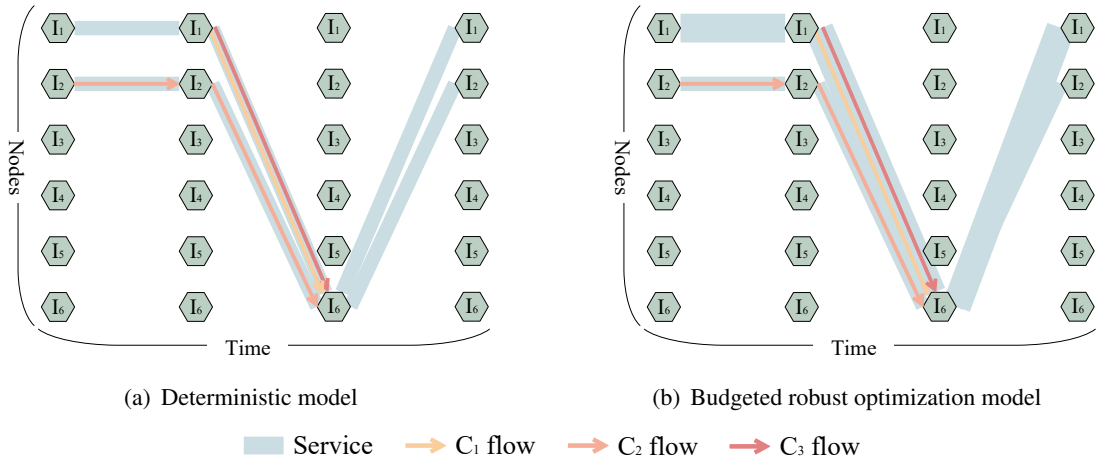

Figure 7. Procurement strategies of the deterministic and budgeted robust optimization models.

To validate the effectiveness of our proposed approach, we compare it with classical budgeted robust optimization model (detailed formulation provided in Appendix B). This model characterizes uncertainty via a polyhedral set that constrains the total scaled deviation of parameters from their nominal values, where the level of conservatism is governed by a budget parameter derived from the regularization term ϑ, identical to the parameter employed in the proposed data-driven uncertainty set. The fundamental difference between the two approaches lies in the uncertainty set construction: Although the budgeted robust optimization model relies on a symmetric geometric structure that may overlook complex data correlations, our proposed SVC-based model constructs a data-driven uncertainty set capable of adaptively capturing arbitrary shapes and dependencies inherent in historical data.

Following the presentation of the data-driven ARO solution, we examine the results yielded by the deterministic model and budgeted robust optimization model. Diverging from the routing configuration of the data-driven ARO model, both the deterministic and budgeted models adopt a distinct V-shaped topological structure centered on Node 6. Specifically, as shown in Figure 7(a), commodities C1, C2, and C3 are transported from their origins at Nodes 1 and 2 to the destination at Node 6, facilitated by the corresponding vehicle service legs. The budgeted robust optimization model, depicted in Figure 7(b), retains this identical topology but significantly augments service capacity to hedge against uncertainty. This resource intensification is represented by the widened service bands along the holding arcs at Node 1 and the return legs, reflecting the increased vehicle deployment defined above. This indicates incurring a higher operational cost to ensure feasibility under worst-case scenarios.

From a cost-efficiency perspective, the data-driven ARO model yields a total operational cost of 1250, whereas the deterministic and budgeted RO models incur costs of 1200 and 1800, respectively. Although the deterministic solution presents the lowest nominal cost, it lacks robustness against demand fluctuations. Specifically, when demand realizes the worst-case scenario within the data-driven uncertainty set (where demands for C_2 and C_3 equal 13.1), the single vehicle with a 20-unit capacity is rendered insufficient, necessitating outsourcing services. The data-driven ARO model accommodates this realization via dynamic recourse, directing the second vehicle to converge with the first. This coordination aggregates capacities to fulfill demand requirements under the worst-case realization defined by the SVC-based uncertainty set. Conversely, the budgeted robust optimization model incurs the highest cost attributable to the geometric looseness of the uncertainty set. As characterized in Remark 3.2, the budgeted set encompasses vacant regions lacking historical data support. To hedge against these theoretical scenarios, the model preemptively deploys three vehicles, which results in resource redundancy.

This comparative analysis underscores the critical influence of demand uncertainty on optimization strategies. The deterministic formulation remains susceptible to infeasibility and penalty costs under demand fluctuations, whereas the budgeted robust optimization approach necessitates excessive resource allocation to ensure comprehensive coverage. By characterizing uncertainty features via historical data, the proposed data-driven ARO model maintains feasibility under worst-case scenarios defined within the uncertainty set. Consequently, this approach mitigates the conservatism inherent in traditional robust optimization, offering a framework that balances system robustness with economic efficiency.

6.2. A practical case

The Western Township Joint Distribution Center in Yuhang, Hangzhou, was selected as a practical case study. This is a real operational setting in which unmanned delivery vehicles are already deployed for intracity last-mile distribution. Empirical data indicates that this facility processes an average daily volume of 160,000 packages, utilizing a fleet of 34 autonomous vehicles that accounts for approximately 35% of total delivery tasks. Regarding vehicle specifications, the predominant model features a capacity of five cubic meters, accommodating a minimum of 300 packages per trip. Therefore, Yuhang is an existing deployment context where our model can be applied to explain and optimize service network design decisions under uncertain demand. We selected ten distribution outlets served by the center as nodes, the geographical locations of which are illustrated in Figure 8 (sourced from Bing Maps). The calculation of the transportation cost for each arc relies on the geographical distance between the origin and destination nodes. For connections between distinct locations, the cost is computed as the product of this distance and

a unit transportation coefficient (u). In cases where the origin and destination coincide, a fixed constant is applied to account for the intranode handling cost associated with internal processing tasks.

Figure 8. Geographical distribution of the selected network nodes in Yuhang, Hangzhou.

6.2.1. Sensitivity analysis of uncertainty set size

To evaluate the performance of the proposed robust optimization model under varying degrees of uncertain risk, we conduct a sensitivity analysis regarding the regularization parameter ϑ. This parameter serves as an upper bound on the proportion of outliers, providing a data-driven mechanism to calibrate the conservatism of the uncertainty set. The experimental analysis focuses on two primary dimensions.

First, we examine the variation of the model's objective value, which represents the total operational cost, across different values of ϑ. As illustrated in Figure 9(a), the objective value exhibits a distinct monotonically decreasing trend as ϑ increases from 0.05 to 0.45. This observation aligns with the theoretical definition of the uncertainty set. Specifically, a higher value of ϑ implies a lower confidence level $(1 - \vartheta)$, which effectively shrinks the uncertainty set by excluding a larger proportion of potential outliers. Consequently, as the model guards against a narrower range of worst-case scenarios, it necessitates fewer resources to ensure feasibility, thereby reducing the total operational cost.

Second, to quantify the cost premium incurred to guarantee conservation, we calculate the price of robustness. As depicted in Figure 9(b), the robust price demonstrates a negative correlation with ϑ. At a low ϑ level (e.g., 0.05), the model enforces a high confidence level (95%), resulting in a larger uncertainty set and a significant robust price. However, as ϑ increases to 0.45, the robust price declines substantially. This result quantitatively underscores the inherent trade-off between system conservation and economic efficiency, as a stricter requirement for uncertain risk coverage (lower ϑ) inevitably requires a higher operational expenditure.

Thirdly, we further decompose the total cost into transportation costs and penalty costs. Figure 10 reports both components under different values of the regularization parameter ϑ, which controls the size of the SVC-based uncertainty set. When ϑ is small, the uncertainty set is larger, and so the protection requirement is more conservative. The model provisions more internal capacity through the first-stage service frequencies, which leads to higher transportation costs, whereas the penalty costs remain relatively low. When ϑ increases, the uncertainty set shrinks, and the protection requirement becomes less conservative. The model reduces internal capacity provisioning, which decreases transportation

costs and increases the penalty costs. This decomposition quantifies how the uncertainty-set size shifts expenditures between internal transportation and outsourcing.

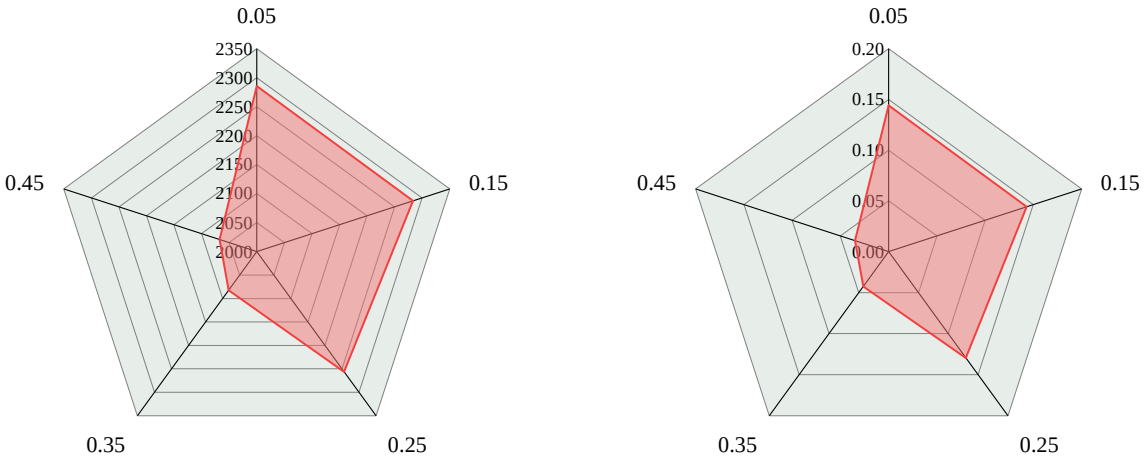

(a) Objective value (b) Robust price

Figure 9. The objective value and robust price of the proposed model under different sizes of the uncertain set.

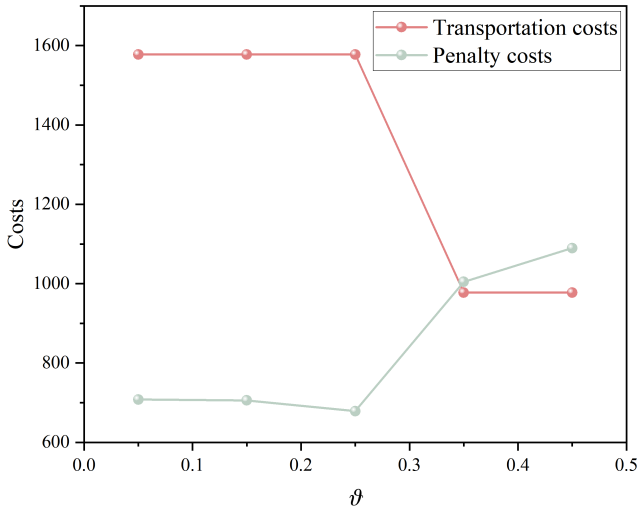

Figure 10. Transportation and penalty cost trade-off under different uncertainty set sizes.

6.2.2. Sensitivity analysis of transportation costs

To investigate the impact of transportation expenses on the optimal operational strategy, we conduct a sensitivity analysis regarding the unit transportation coefficient u. The experiments consider two distinct scenarios for the outsourcing cost α to evaluate how the trade-off between internal transportation and external outsourcing evolves.

As illustrated in Figure 11(a), where the outsourcing cost is relatively low ($\alpha = 0.05$), the total cost initially rises in tandem with u. However, a significant structural shift occurs when u increases from 2 to 3. At this threshold, the outsourcing volume exhibits a sharp surge, whereas the growth of the total

cost notably decelerates and stabilizes. This behavior indicates a substitution effect. Specifically, when the internal unit transportation cost exceeds a critical level relative to the low outsourcing price, the model strategically shifts a majority of the workload to external carriers to mitigate the overall financial burden. Conversely, Figure 11(b) depicts the scenario with a higher outsourcing cost ($\alpha = 0.08$). Here, the system exhibits a stronger reliance on the internal fleet. The outsourcing volume remains minimal for a wider range of u (from 1 to 4), and the total cost continues to climb steeply without flattening. The shift to outsourcing is delayed until u reaches 5. This comparison quantitatively reveals that a higher outsourcing cost raises the threshold for activating external resources, as the system prefers to absorb the increasing internal transportation costs rather than pay the expensive outsourcing fee.

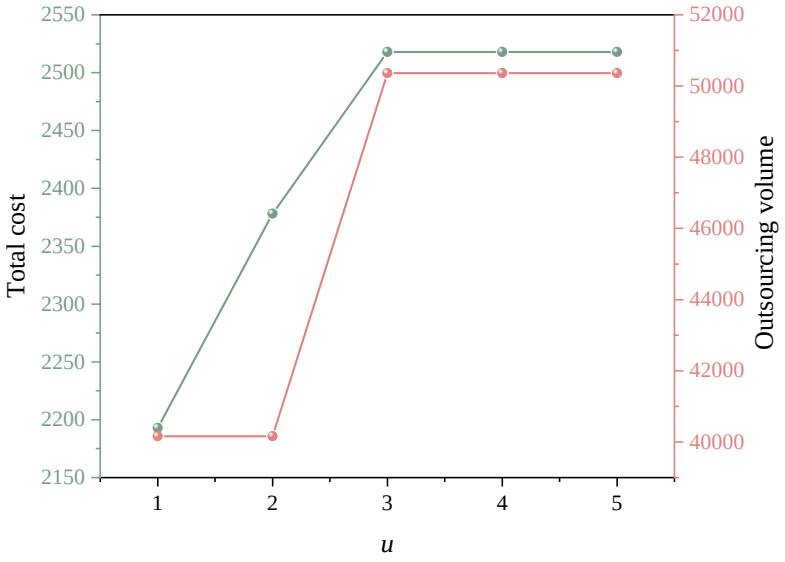

(a) α=0.04

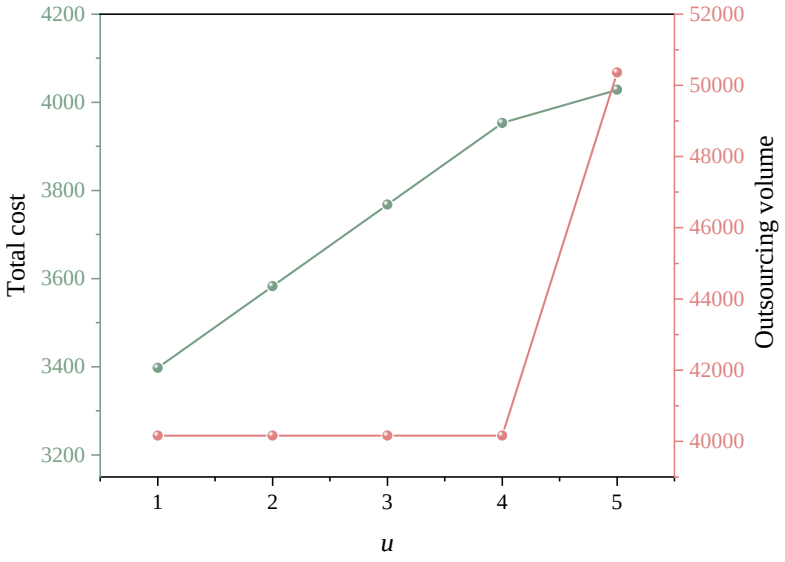

(b) α=0.07

Figure 11. Impact of the unit transportation coefficient u on the total cost and outsourcing volume with varying outsourcing costs α.

6.2.3. Sensitivity analysis of vehicel capacity

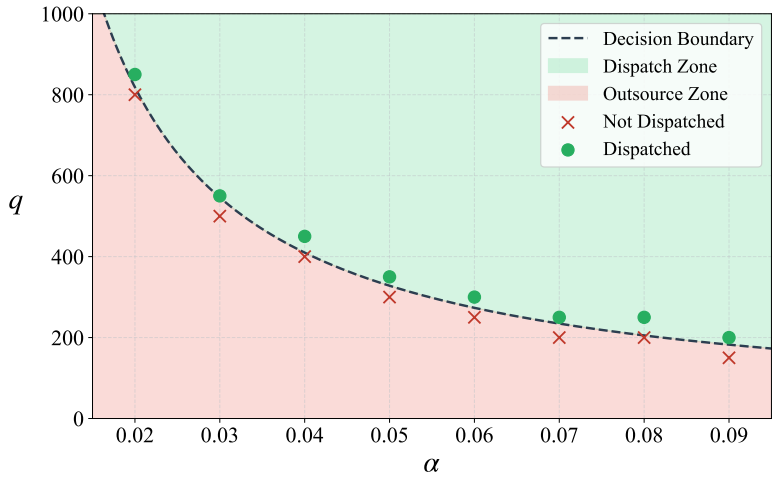

Figure 12. Economic feasibility boundaries for vehicle capacity under varying market rates.

To investigate the influence of physical resource limitations on operational efficiency, we conduct a sensitivity analysis regarding vehicle capacity q. The experimental results are visualized in Figure 12, which defines the minimum capacity threshold required for the internal fleet to remain cost-effective against varying market rates. The decision boundary partitions the solution space into a dispatch zone, where the vehicle capacity is sufficient to justify self-operation, and an outsource zone, where capacity constraints render outsourcing the more economical choice. The analysis reveals that the required vehicle capacity is inversely correlated with the external outsourcing cost. When the market price for outsourcing is low ($\alpha = 0.02$), the system demands a substantial vehicle capacity of approximately 800 to efficiently amortize internal operational costs and compete with the inexpensive external option. Conversely, as the market rate rises to 0.09, the capacity threshold for internal dispatching declines significantly to a range between 150 and 200. This observation indicates that the comparative economic advantage of internal dispatching becomes more pronounced as the external market becomes more expensive. Consequently, under high outsourcing cost scenarios, vehicles with smaller capacities gain economic viability for internal dispatching, whereas strictly high-capacity vehicles are required to maintain cost advantages when external prices are low.

6.2.4. Sensitivity analysis of historical data size

Given that the uncertainty set $\mathscr{D}(\boldsymbol{d})$ is derived from historical demand samples via SVC, this section examines the sensitivity of the model to data availability. We vary the historical sample size N utilized to construct $\mathscr{D}(\boldsymbol{d})$, maintaining all other parameters constant. For each sample size N, we generate the uncertainty set using Algorithm 1 and solve the data-driven ARO model to determine the optimal total cost. The analysis considers three regularization parameter values: $\vartheta \in \{0.05, 0.15, 0.25\}$. Figure 13 presents the results. Across all ϑ levels, the objective value declines as N increases from 50 to 100 and subsequently stabilizes as N exceeds 150. These observations indicate that incorporating additional historical data refines the learned uncertainty set and mitigates the conservatism of the objective value, with the solution quality converging once the sample size reaches a moderate scale.

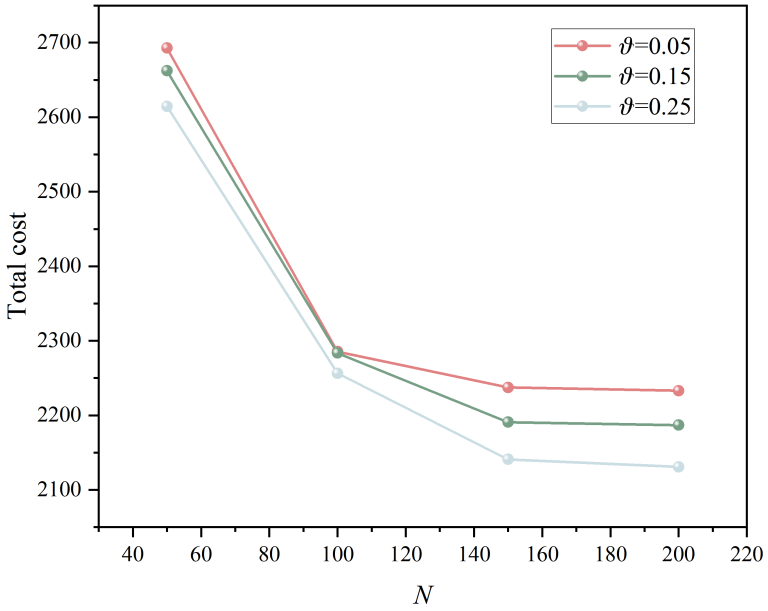

Figure 13. Sensitivity of the objective value to the historical data size N.

6.3. Practical implementation considerations

This subsection discusses practical aspects of deploying our proposed data-driven ARO framework, covering data availability, computational requirements, and integration with real-time logistics platforms.

From a data perspective, our proposed framework relies on information that is routinely collected in express delivery operations. Specifically, it requires: (i) time-stamped order records that can be aggregated into commodity level demand samples $\{\boldsymbol{d}^{(n)}\}_{n=1}^{N}$ over the discretized periods, typically available from order management systems and enterprise resource planning databases; (ii) network topology and arc attributes, including internode distances and time-dependent travel times, which are used to compute arc transportation costs and are typically obtained from transportation management systems, routing engines, and map services; and (iii) operational parameters, including vehicle capacity q, candidate departure schedules, node handling or waiting costs (for holding arcs), and time-window parameters (γ_c, τ_c), which are commonly maintained in fleet management systems, warehouse management systems, and service-level agreement records. These inputs are aligned to the time-space network representation adopted in the model.

From a computational perspective, our proposed data-driven ARO formulation involves semi-infinite constraints induced by the SVC-based uncertainty set. To render the problem tractable, we apply linear decision rules to parameterize recourse variables as affine functions of the uncertain demands and then use duality theory to reformulate the resulting worst-case terms. This yields an equivalent tractable robust counterpart in the form of a mixed-integer linear program. This reformulation can be solved using the customized Benders dual decomposition algorithm.

In terms of platform integration, the first-stage decision $X_{ii'}(t)$ specifies the planned service frequencies on the time-space network, which translate into dispatch schedules and baseline fleet allocation over the planning horizon. During execution, real-time order arrivals instantiate realized demands $d_c(t)$, and the recourse layer determines the flow allocations $Y_{ii'c}(t)$ subject to capacities $qX_{ii'}(t)$ and time windows (γ_c, τ_c), thereby routing shipments through sorting and transportation legs. When

capacity is insufficient on specific arcs or periods, our model activates outsourcing via $Z_c(t)$ by assigning unmet demand to external carriers. The uncertainty set can be updated periodically using newly observed demand data, the baseline plan $X_{ii'}(t)$ can be reoptimized at a managerial cadence, and the recourse decisions (Y, Z) can be executed in a rolling-horizon manner using current system states such as fleet availability and time-dependent travel times.

7. Conclusions and future research

In this study, we addressed the service network design problem for capacity-constrained intracity express delivery systems by proposing a data-driven ARO framework. By integrating SVC to construct the uncertainty set and employing a customized Benders dual decomposition algorithm, this research can effectively bridge the gap between theoretical robust modeling and practical logistics operations under demand uncertainty.

The numerical experiments yield critical managerial insights into the interplay between conservation, sourcing costs, and resource configurations. First, regarding conservation, the analysis demonstrates that the regularization parameter ϑ serves as a pivotal lever for balancing system robustness and economic efficiency. We observe a negative correlation between ϑ and the robust price, which suggests that managers must accept a higher cost premium to achieve greater protection against worst-case demand fluctuations. Second, regarding outsourcing strategies, we identify a threshold-based substitution effect. The results indicate that rising external market rates significantly elevate the threshold for outsourcing, implying that firms should prioritize internal fleets and tolerate higher internal costs before resorting to expensive external carriers. Third, regarding vehicle selection, the study reveals that the economic viability of vehicle capacity is dynamic rather than static. High outsourcing costs enhance the comparative economic advantage of internal dispatching. Consequently, even vehicles with smaller capacities gain economic viability for internal operations when facing expensive external alternatives, whereas strictly high-capacity vehicles are required to maintain cost advantages when external prices are low. The proposed framework provides logistics practitioners with a robust decision support tool that ensures solution feasibility against demand uncertainty.

Although the numerical experiments validate the effectiveness of our proposed approach, there are still limitations. First, the reliance on linear decision rules to reformulate the adaptive robust model may introduce an optimality gap compared to fully adjustable policies. Future research could explore more flexible mechanisms, such as piecewise linear decision rules, to further improve solution quality. Second, this study primarily focuses on economic costs. Given the growing importance of sustainable logistics, extending the current framework to a multiobjective optimization model that simultaneously accounts for carbon emissions and service reliability represents a promising direction for further study.

Author contributions

Shijun Wang: Conceptualization, Methodology, Writing - Original draft preparation, Software, Data curation, Validation. **Yanjiao Wang:** Conceptualization, Methodology, Writing - Review & Editing, Software, Data curation. **Naiqi Liu:** Writing - Review & Editing, Visualization, Funding acquisition. **Weida Zhang:** Writing - Review & Editing, Project administration.

Use of Generative-AI tools declaration

In the preparation of this work, the authors used Generative AI tools such as ChatGPT to assist in improving the clarity of the language. All AI-assisted content was carefully reviewed and revised by the authors, who take full responsibility for the final version of the manuscript.

Acknowledgments

The authors gratefully acknowledge the insightful comments received from the editors and anonymous referees, which have considerably improved the quality of the paper. This work was supported by the National Natural Science Foundation of China (No. 72471164) and the Post-Graduate's Innovation Fund Project of Hebei University (No. HBU2024SS006).

Conflict of interest

All authors declare no conflicts of interest in this paper.

References

1. I. Dayarian, A. Rocco, A. Erera, M. Savelsbergh, Operations design for high-velocity intra-city package service, *Transp. Res. Part B Methodol.,* **161** (2022), 150–168. https://doi.org/10.1016/j.trb.2022.05.002
2. Y. H. Wu, H. Fang, A. G. Qureshi, T. Yamada, Capacitated hub location routing problem with time windows and stochastic demands for the design of intra-city express systems, *Eur. J. Oper. Res.,* **326** (2025), 255–269. https://doi.org/10.1016/j.ejor.2025.05.006
3. X. P. Wang, J. L. Zhao, Distributionally robust optimization of the vehicle routing problem with uncertain customers, *J. Ind. Manag. Optim.,* **21** (2025), 1983–2006. https://doi.org/10.3934/jimo.2024159
4. State post bureau of the People's Republic of China, 2024 Postal industry development statistical bulletin, 2025. Available from: https://www.spb.gov.cn/gjyzj/c100276/202501/460d02f2e54c4d0ebbba3a4f431d0042.shtml.
5. C. Liu, J. J. Zhou, J. W. Gan, Y. X. Wu, Y. L. Huang, J. H. Shao, et al., Optimizing the ground intra-city express delivery network: An integrated multiple centrality assessment, multi-criteria decision-making, and multi-objective integer programming model, *J. Intell. Transp. Syst.,* **28** (2024), 525–543. https://doi.org/10.1080/15472450.2022.2157211
6. X. Chu, S. W. Chen, K. Wang, L. X. Wu, G. Y. Xu, A cost-efficiency analysis of drones in revolutionizing intra-city express services, *Adv. Eng. Inform.,* **65** (2025), 103324. https://doi.org/10.1016/j.aei.2025.103324
7. M. Seifbarghy, F. Yargholi, M. Hamidi, Modeling a stochastic multi-objective, multi-site, multi-mode, and multi-item supplier selection and order allocation problem, *J. Ind. Manag. Optim.,* **20** (2024), 2980–3003. https://doi.org/10.3934/jimo.2024037

8. R. Diaz, C. Phan, D. Golenbock, B. Sanford, A prescriptive framework to support express delivery supply chain expansions in highly urbanized environments, *Ind. Manag. Data Syst.,* **122** (2022), 1707–1737. https://doi.org/10.1108/IMDS-02-2022-0076

9. L. B. Guo, X. T. Guo, Y. J. Wang, Decision-making for demand signal in crowd sourcing platform, *J. Ind. Manag. Optim.,* **20** (2024), 664–678. https://doi.org/10.3934/jimo.2023096

10. Y. J. Wang, A. X. Chen, N. Q. Liu, Constructing resilient supply chain for risk-averse buyers by data-driven robust optimization approach, *Int. J. Prod. Econ.,* (2025), 109734. https://doi.org/10.1016/j.ijpe.2025.109734

11. H. Mollashahi, Optimization of closed-loop supply chains with a waste management and recycling approach: examining the effects of capacity, facility location, and uncertainty management in responding to variable demand, *J. Ind. Manag. Optim.,* **21** (2025), 5435–5453. https://doi.org/10.3934/jimo.2025099

12. R. P. Huang, S. J. Qu, Z. M. Liu, Two-stage distributionally robust optimization model for warehousing-transportation problem under uncertain environment, *J. Ind. Manag. Optim.,* **19** (2023), 6344–6363. https://doi.org/10.3934/jimo.2022218

13. Q. Meng, X. L. Hei, S. A. Wang, H. J. Mao, Carrying capacity procurement of rail and shipping services for automobile delivery with uncertain demand, *Transp. Res. Part E Logist. Transp. Rev.,* **82** (2015), 38–54. https://doi.org/10.1016/j.tre.2015.07.005

14. S. Khalifehzadeh, M. B. Fakhrzad, Y. Z. Mehrjerdi, H. Hosseini_Nasab, Two effective metaheuristic algorithms for solving a stochastic optimization model of a multi-echelon supply chain, *Appl. Soft Comput.,* **76** (2019), 545–563. https://doi.org/10.1016/j.asoc.2018.12.018

15. M. Q. Yin, M. Huang, X. W. Wang, L. H. Lee, Fourth-party logistics network design under uncertainty environment, *Comput. Ind. Eng.,* **167** (2022), 108002. https://doi.org/10.1016/j.cie.2022.108002

16. D. Petrovic, M. Kalata, J. Luo, A fuzzy scenario-based optimisation of supply network cost, robustness and shortages, *Comput. Ind. Eng.,* **160** (2021), 107555. https://doi.org/10.1016/j.cie.2021.107555

17. Y. Sun, Fuzzy approaches and simulation-based reliability modeling to solve a road–rail intermodal routing problem with soft delivery time windows when demand and capacity are uncertain, *Int. J. Fuzzy Syst.,* **22** (2020), 2119–2148. https://doi.org/10.1007/s40815-020-00905-x

18. J. Q. Guo, L. Chen, Configuration and optimisation of a green closed-loop supply chain with delivery time and green investment considering government subsidy under meta-heuristics algorithms, *Int. J. Syst. Sci. Oper. Logist.,* **11** (2024), 2401033. https://doi.org/10.1080/23302674.2024.2401033

19. X. Xiang, T. Fang, C. C. Liu, Z. Pei, Robust service network design problem under uncertain demand, *Comput. Ind. Eng.,* **172** (2022), 108615. https://doi.org/10.1016/j.cie.2022.108615

20. E. Taniguchi, M. Noritake, T. Yamada, T. Izumitani, Optimal size and location planning of public logistics terminals, *Transp. Res. Part E Logist. Transp. Rev.,* **35** (1999), 207–222. https://doi.org/10.1016/S1366-5545(99)00009-5

21. J. Nicholson, F. Gzara, A. Alnaggar, Unmanned aerial vehicle traffic network design with risk mitigation, *Transp. Res. Part E Logist. Transp. Rev.,* **204** (2025), 104380. https://doi.org/10.1016/j.tre.2025.104380

22. O. Satici, I. Dayarian, Tactical and operational planning of express intra-city package services, *Omega,* **122** (2024), 102940. https://doi.org/10.1016/j.omega.2023.102940

23. X. Wang, L. Wang, C. X. Dong, H. Ren, K. Xing, An online deep reinforcement learning-based order recommendation framework for rider-centered food delivery system, *IEEE Trans. Intell. Transp. Syst.,* **24** (2023), 5640–5654. https://doi.org/10.1109/TITS.2023.3237580

24. A. Behrendt, M. Savelsbergh, H. Wang, A prescriptive machine learning method for courier scheduling on crowdsourced delivery platforms, *Transp. Sci.,* **57** (2023), 889–907. https://doi.org/10.1287/trsc.2022.1152

25. A. Ben-Hur, D. Horn, H. T. Siegelmann, V. Vapnik, Support vector clustering, *J. Mach. Learn. Res.,* **2** (2001), 125–137.

26. C. Shang, X. L. Huang, F. Q. You, Data-driven robust optimization based on kernel learning, *Comput. Chem. Eng.,* **106** (2017), 464–479. https://doi.org/10.1016/j.compchemeng.2017.07.004

27. A. Ben-Tal, L. El Ghaoui, A. Nemirovski, *Robust Optimization*, Princeton University Press, Princeton, 2009.

28. M. Bodur, J. R. Luedtke, Two-stage linear decision rules for multi-stage stochastic programming, *Math. Program.,* **191** (2022), 347–380. https://doi.org/10.1007/s10107-018-1339-4

29. S. J. Garstka, R. J. B. Wets, On decision rules in stochastic programming, *Math. Program.,* **7** (1974), 117–143. https://doi.org/10.1007/BF01585511

30. R. Rahmaniani, S. Ahmed, T. G. Crainic, M. Gendreau, W. Rei, The Benders dual decomposition method, *Oper. Res.,* **68** (2020), 878–895. https://doi.org/10.1287/opre.2019.1892

31. S. J. Wang, Y. Lu, F. Chu, J. B. Yu, Scheduling with divisible jobs and subcontracting option, *Comput. Oper. Res.,* **145** (2022), 105850. https://doi.org/10.1016/j.cor.2022.105850

32. A. G. Lium, T. G. Crainic, S. W. Wallace, A study of demand stochasticity in service network design, *Transp. Sci.,* **43** (2009), 144–157. https://doi.org/10.1287/trsc.1090.0265

AIMS Press